



# Predicted Dark Energy Constraints using 3D Weak Lensing

T. D. Kitching

Institute for Astronomy, University of Edinburgh, Royal Observatory, Blackford Hill, Edinburgh, EH9 3HJ, United Kingdom

**Abstract.** I hereby present two different methods that will allow weak lensing shape measurements of galaxies combined with redshift information – 3D weak lensing – to constrain the dark energy equation of state. The two methods are the geometric ratio test (Taylor et al. 2007) and a shear harmonic test (Heavens et al. 2006). The results presented here use a Fisher matrix approach for each method to place lower limits on the expected cosmological parameter constraints from future weak lensing surveys combined with a predicted Planck CMB prior, fully marginalizing over all cosmological parameters and allowing for spatial curvature. The parameter estimation technique allows for an optimisation of future experiments so that the dark energy parameter constraints, given a specific amount of time on a particular instrument, can be minimised.

## 1. Introduction

There is now overwhelming evidence that the isotropic expansion of the Universe is accelerating (for example Spergel et al. 2006). This acceleration has been attributed to a negative pressure component of the mass-energy content of the Universe, accounting for approximately 70% of the total mass-energy. The identity of this component remains a mystery, and so to maintain ambiguity has been labelled ‘dark energy’. There are a menagerie of possible physical phenomenon that could exhibit a negative pressure. The simplest being a new feature of gravity, manifest on large scales, for example a cosmological constant. Alternative gravity theories also attempt to explain dark energy by modifying the Friedmann equation. The alternative to a gravity-based explanation attributes dark energy to the latent energy of the vacuum. Most theories of this form propose a pervading scalar field with a slow roll potential. These quintessence fields are akin to Inflationary scalar fields. The standard model of particle physics predicts a vacuum energy. By summing the zero-energy values of all the known fields, the approximate value is  $10^{120}$  times larger than current cosmological constraints. So, the determination of the nature of dark energy has the potential to help in solutions within particle physics as well as cosmology.

The simplest model for an ambiguous dark energy component can be parameterized by an equation of state

$$p_{\text{de}} = w c^2 \rho_{\text{de}}. \quad (1)$$

A cosmological constant would have a non-varying,  $w = -1$ , equation of state, whereas a quintessence-type explanation would have some dynamical redshift evolution  $w = w(z)$ . It is the determination of the equation of state of dark energy that will allow an inference about its nature to be made. Here the most common expansion of  $w(z)$  will be made (Linder 2003)

$$w(z) = w_0 + w_a \left( \frac{z}{1+z} \right), \quad (2)$$

where  $w_0$  is the present day value of the equation of state and  $w_a$  encodes its redshift evolution. The pair of parameters,  $w_0$  and  $w_a$ , can be used to describe, and distinguish between, a wide class of possible, smoothly varying, dark energy evolutionary tracks. To place constraints on the dark energy equation of state parameters cosmological probes need to be ‘three-dimensional’. Since the effect of dark energy is an acceleration (over time), probes which study its effect necessarily need to gain information on the expansion history at a variety of redshifts.

Current observations (Spergel et al. 2006) have constrained the dark energy equation of state to be approximately akin to a cosmological constant, although in order to convincingly distinguish between competing models tighter constraints on both  $w_0$  and  $w_a$  are needed. There are a plethora of proposed future experiments including both spaced based (for example SNAP, Aldering 2005) and ground based large multi-band optical and infrared surveys, wide field spectroscopic surveys (for example WFMOS, Bassett et al. 2005), and CMB experiments all of which will provide complimentary dark energy constraints. Here I will consider a 5 band ground based optical survey covering 10,000 square degrees to a median redshift of  $z_m = 0.7$ , which may be achievable by dark-CAM (Taylor 2005) and the Dark Energy Survey (DES) (Wester 2005). A predicted CMB prior from the proposed Planck satellite (Lamarre et al. 2003), which will be contemporary with such a ground based experiment, will also be included.

Weak lensing can probe both the geometry of the Universe via the observer-lens-source distance relations and the growth of structure via the integral effect of distant galaxies being lensed by intervening large scale structure. Lensing is attractive as a dark energy probe, as the methods rely only on well understood and simple physical effects i.e. general relativity.

The image of a background galaxy will be slightly distorted by any intervening mass distribution. The pattern

induced by this gravitational lensing on a galaxies shape can be expressed in terms of a complex shear

$$\gamma(\theta) = \gamma_1(\theta) + i\gamma_2(\theta), \quad (3)$$

where  $\gamma_1$  and  $\gamma_2$  represent distortions in orthogonal directions at an angle  $\theta$ . 3D weak lensing uses the shear information *and* any redshift information available (either photometric or spectroscopic) for every galaxy. The geometric ratio test will use the distortions produced by a large intervening mass such as a galaxy cluster, where as the shear harmonic test uses the distortions produced by large scale structure (cosmic shear).

Section 2 will present details of the geometric ratio test. Section 3 will present details the shear harmonic test. The survey design formalism and predicted cosmological constraints from both methods will be presented in Section 4. Conclusions are presented in Section 5.

## 2. Geometric Ratio Test

The geometric ratio test, an adaption of the Jain & Taylor (2003) shear-ratio test, uses the shear distortion induced on background galaxies by an intervening galaxy cluster. A circular symmetric galaxy cluster should produce distortions that are perpendicular to the line from a background galaxy image to the center of the cluster i.e. a tangential distortion. In this case it is convenient to use the tangential shear, projected out from the total shear given in equation (3),

$$\gamma_t = -[\gamma_1 \cos(2\phi) + \gamma_2 \sin(2\phi)] \quad (4)$$

where  $\phi$  is the azimuthal angle around the center of the cluster. The amplitude of the induced distortion grows with redshift behind a cluster so that the induced distortion of a galaxy at a particular redshift is

$$\gamma_t(z) = \gamma_\infty \frac{S_k[r(z) - r(z_l)]}{S_k[r(z)]} \quad (5)$$

where  $\gamma_\infty$  depends on the mass profile of the cluster,  $z_l$  is the redshift of the cluster,  $r(z)$  is the comoving distance and  $S_k(r) = r_0 \sin(r_0/r)$ ,  $r$ ,  $r_0 \sinh(r_0/r)$  for  $k = 1, 0, -1$  encodes any curvature information. By taking the ratio of  $\gamma_t$  at two different redshifts the mass dependence of the signal is cancelled so that the geometric ratio for two different redshifts  $z_i$  and  $z_j$  for a given cluster is

$$R_{ij} = \frac{\gamma_t(z_i)}{\gamma_t(z_j)} = \frac{S_k[r(z_i) - r(z_l)]S[r(z_j)]}{S_k[r(z_j) - r(z_l)]S[r(z_i)]}. \quad (6)$$

This ratio only depends on the geometric cosmological parameters through the comoving distance relation;  $\Omega_m$ ,  $\Omega_{de}$ ,  $w_0$  and  $w_a$ . Photometric redshifts are included by taking into account the change in both the redshift dependence of the tangential shear profile and the number density distribution, see Taylor et al. (2007).

Compressing the notation for a pair of background galaxies  $\mu = (i, j)$  and  $\nu = (m, n)$  the log-likelihood for a particular survey is the sum of the log-likelihoods for

each individual cluster. The Fisher matrix is given by (see Taylor et al. 2007)

$$F_{ij} = \frac{1}{2} \sum_{\mu, \nu} (\partial_i R_\mu [C_{\mu\nu}^{RR}]^{-1} \partial_j R_\nu + \partial_j R_\mu [C_{\mu\nu}^{RR}]^{-1} \partial_i R_\nu), \quad (7)$$

where  $\partial_i$  is a derivative with respect to a cosmological parameter. The covariance terms,  $C_{\mu\nu}^{RR}$ , contain terms for shot noise due to the intrinsic dispersion in galaxy shapes, and a cosmic shear term due to large scale structure between the source galaxies and the observer, these are given in Taylor et al. (2007).

The the number of clusters as a function of mass and redshift,  $N(M, z)$ , was accurately modelled using a halo decomposition of the matter field. The Sheth-Torman form for the fraction of matter in halos of a given mass was used. A lower cut-off in the mass of clusters, at any given redshift, was set so that cluster shear must be measurable with  $\Delta\gamma/\gamma > 1$ .

## 3. Shear Harmonic Test

The shear harmonic test uses every galaxy in a survey as an estimator of the underlying 3D shear field. This field can be devolved using a spherical harmonic expansion, see Heavens (2003), Heavens et al. (2006) and Castro et al. (2005), where the expansion coefficients are calculated by summing over all galaxies,

$$\hat{\gamma}_i(k, \underline{\ell}) = \sqrt{\frac{2}{\pi}} \sum_g \gamma_i^g j_\ell(kr_0^g) e^{-i\underline{\ell} \cdot \underline{\theta}} \quad (8)$$

where the  $\gamma_i^g$  are the components given in equation (3) where  $i = (1, 2)$ ,  $\underline{\theta}$  is the position of each galaxy  $g$ , the  $j_\ell(z)$  are spherical Bessel functions and the subscript 0 refers to a fiducial cosmology.  $k$  is the radial wavenumber, and  $\underline{\ell} = (\ell_x, \ell_y)$  is the angular wavenumber on the sky.

By representing the expected shear field at a given redshift and position by the integrated, scaled, lensing potential along the line of sight due to large scale structure the expected coefficients of the devolved shear field can be related, via Poisson's equation, to the integrated matter overdensity along the line of sight. The covariance of the coefficients depends on the matter power spectrum. The shear harmonic test depends not only on the geometric parameters but on the parameters that determine both the shape and evolution of the matter power spectrum. Dark energy dependent growth factors from Linder (2003) are used in the analysis. The parameter set used here is  $(\Omega_m, \Omega_v, h, \sigma_8, \Omega_b, w_0, w_a, n_s, \alpha_n)$ . Photometric redshifts are included by convolving the coefficients with a Gaussian in redshift with a variance given by equation (10).

A shot noise term is included by replacing the above sum in equation (8) by a sum of cells containing either 1 or 0 galaxies see Heavens et al. (2006). The covariance matrix,  $C$ , is the sum of the signal covariance matrix, given by taking the covariance of equation (8), and the shot noise matrix.

The Fisher matrix is calculated by summing over all angular modes

$$F_{ij} = \frac{1}{2} \sum_{\ell} \text{Trace}[(C^{\ell})^{-1} C^{\ell}_{,i} (C^{\ell})^{-1} C^{\ell}_{,j}] \quad (9)$$

where a comma represents the derivative with respect to a cosmological parameter.

## 4. Results

The photometric redshift accuracies and number density profiles, common to both methods will be addressed in Section 4.1. In Section 4.2 the CMB prior used will be introduced. The fiducial cosmology used in all the Fisher matrix calculations is  $\Omega_m = 0.27$ ,  $\Omega_v = 0.73$ ,  $h = 0.71$ ,  $\sigma_8 = 0.80$ ,  $\Omega_b = 0.04$ ,  $w_0 = -1.0$ ,  $w_a = 0.0$ ,  $n_s = 1.0$ ,  $\alpha_n = 0.0$ ,  $\tau = 0.09$ ,  $r = 0.01$ .

### 4.1. Survey Design

Photometric redshift uncertainties were accurately modelled using a redshift and magnitude dependent form for the error at a particular redshift. For a 5 band survey this is given by (Taylor et al. 2007)

$$\sigma_z(z, R) = 0.035(1+z)(1+10^{0.8(R-23.0)}) \quad (10)$$

where  $R$  is the absolute magnitude of a galaxy. Equation (10) was then integrated over magnitude using redshift dependent Schechter luminosity functions taken from the COMBO-17 survey. The resulting photometric redshift error form can be approximately fitted by the following form

$$\sigma_z(z) \approx 0.063(0.64+z). \quad (11)$$

This has a slightly higher gradient than the standard  $\sigma_z(z) = 0.05(1+z)$  usually used for 5-band survey predictions, with values lower at  $z \lesssim 0.7$  and higher at  $z \gtrsim 0.7$ .

A functional form for the background galaxy redshift distribution was assumed to be

$$n(z|z_m) = n_0 \frac{2z_*^3}{3} z^2 \exp[-(z/z_*)^{1.5}] \quad (12)$$

where  $z_* = z_m/1.412$  and  $n_0$  is the number of galaxies per square arcminute on the sky given by  $n_0 = 30z_m^{3.4}$ . A maximum redshift of  $z = 1.5$  is assumed as ground based ellipticity measurements cannot be made at redshifts beyond this.

In Section 4.3 the results of optimising a future wide field survey will be presented. Optimisation, in this sense, means given a certain number nights  $T$  on a given instrument, choosing the survey strategy that will result in the minimum error on a particular parameter, in this case  $w_0$ , being achieved. For an imaging survey the time taken on a given telescope, with diameter  $D$  and field of view  $F$ , to image down to a median redshift  $z_m$  over an area  $A$  scales as

$$T \propto z_m^4 f_{\text{sky}} D^{-2} F^{-1} \quad (13)$$

where  $f_{\text{sky}} = A/(40,000 \text{ square degrees})$ , the constant of proportionality has to be taken from an existing survey as shown in Taylor et al. (2007). Given a specific telescope and instrument the question then becomes: ‘‘Should the survey be wider (large area) and shallower (low  $z_m$ ) or narrower and deeper?’’

### 4.2. Predicted CMB Prior

A predicted 14-month Planck prior was calculated using CMBfast (version 4.5.1, Seljak & Zaldarriaga 1996). The Fisher matrix for a CMB experiment is

$$F_{ij}^{CMB} = \sum_{\ell_{\min}}^{\ell_{\max}} \sum_{X,Y} \frac{\partial C_{X\ell}}{\partial \theta_i} (\text{Cov}_{\ell})_{XY}^{-1} \frac{\partial C_{Y\ell}}{\partial \theta_j} \quad (14)$$

where  $C_{X\ell}$  is the power for  $X = T, E, TE$  or  $B$  (Temperature, E channel polarization, Temperature-E channel cross correlation and B channel polarization) in the  $\ell^{\text{th}}$  multipole. The elements of the symmetric covariance matrix were taken from Eisenstein et al. (1998) and the Planck survey parameters from Hu (2002). The maximum multipole used was  $\ell_{\max} = 2000$  and a minimum of  $\ell_{\min} = 10$ , the sky fraction assumed was  $f_{\text{sky}} = 0.66$  which simulates a typical galactic cut. The 11-parameter CMB cosmological parameter set used was  $(\Omega_m, \Omega_v, h, \sigma_8, \Omega_b, w_0, w_a, n_s, \alpha_n, \tau, r = T/S)$ . A marginalization over calibration of the CMB instrument was not included.

### 4.3. Parameter Constraints

Figure 1 shows the parameter constraints in the  $(w_0, w_a)$  plane for the fiducial survey design of  $z_m = 0.70$  and  $A = 10,000$  square degrees. It can immediately be seen that the two methods constrain very different areas within this parameter space, and both make at least a factor of 5 improvement on the Planck CMB constraint in combination. The orientation of the ellipse constrained in this parameter space corresponds to a constraint of  $w(z)$  at a particular redshift known as the pivot redshift, the constraint at this redshift corresponding to the narrowest width of the inclined ellipse in the  $(w_0, w_a)$  plane. The pivot redshifts and  $1-\sigma$  pivot redshift constraints for the two methods are shown in Table 1.

It can be seen that the geometric ratio test constrains the dark energy equation of state at a particularly low redshift. This is due to the response of the tangential shear profile to the  $w_a$  parameter, which only effects the expansion rate at large redshifts. Since the shear harmonic test is constraining dark energy via geometric effects and the growth of structure, and the CMB dark energy constraint comes mainly from the large scale ISW effect the pivot redshifts of the two experiments are similar. The geometric ratio and shear harmonic tests are complementary in that they can independently place tight constraints on the evolution of the dark energy equation of state at different redshifts.

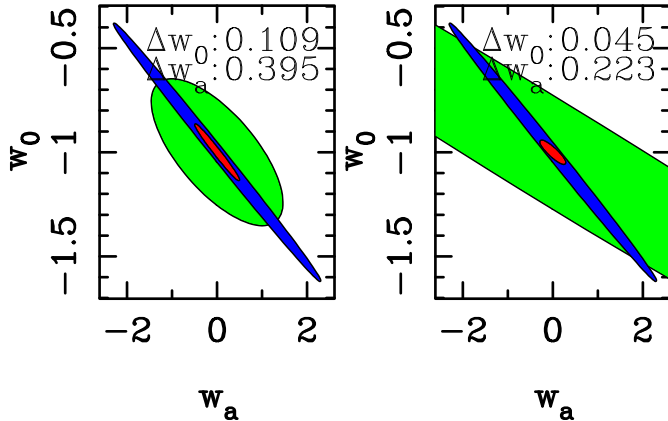


**Fig. 1.** The two parameter  $1\text{-}\sigma$  contours in the  $(w_0, w_a)$  plane for the shear harmonic test (light shaded region, right hand panel) and the geometric ratio test (light shaded region, left hand panel) combined with a 14-month Planck prior (dark shaded regions, both panels) and the combined constraints (central light shaded regions, both panels). The combined marginal errors on  $w_0$  and  $w_a$  are shown for both methods.

**Table 1.** Pivot Redshifts.

Method	$z_{\text{pivot}}$	$\Delta w(z_{\text{pivot}})$
Geometric Ratio Test	0.221	0.0202
Shear Harmonic Test	0.373	0.0175

Figure 2 shows the variation in the marginal error on  $w_0$  given 600 nights on a 4 meter class telescope with a 2 square degree field of view, combined with a Planck prior. The geometric ratio test minimises at  $z_m \approx 0.60$  with  $A \approx 18,500$  square degrees whereas the shear harmonic test minimises at  $z_m \approx 1.00$  with  $A \approx 2400$  square degrees. The differences in the optimal median redshift can be understood in terms of the pivot redshifts being constrained by the particular experiments. The median redshift being approximately three times the pivot redshift so that the line of sight light paths for majority of the background galaxies pass through the redshift range where the response to the dark energy parameters for a particular experiment is maximised.

## 5. Conclusions

The two methods presented here, when applied to future wide field multi-band surveys, will allow the dark energy equation of state parameters to be determined to an unprecedented degree of accuracy. Here it has been shown that the two methods described can improve on CMB constraints by at least a factor of 5. The two methods probe the dark energy equation of state in different ways, the geometric ratio test through geometry and the shear harmonic test through geometry and growth of structure, so that they place minimum constraints at different and complementary pivot redshifts. It has also been shown that

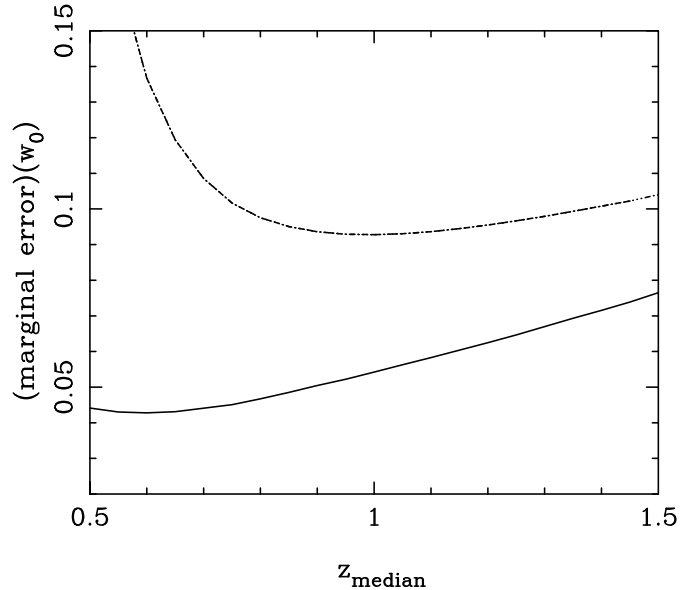


**Fig. 2.** Variation of marginal error on  $w_0$  with median redshift given 600 nights on a 4 meter class telescope with a 2 square degree field of view. The area scales as equation (13) with  $A = 10,000$  square degrees corresponding to  $z_m = 0.70$ . The solid line is for the geometric ratio test, the dot-dashed line is for the shear harmonic test.

when designing a weak lensing survey to measure the dark energy equation of state, the optimisation of the survey strategy can improve constraints by up to 2 times, the optimal median redshift depending on the type of method used. By using such methods the answer to the question: “What is the Universe made of?” will be answered with the next generation of surveys.

*Acknowledgements.* This work was supported by a PPARC studentship. I would like to thank Alan Heavens and Andy Taylor for help at every stage of this work. I would also like to thank David Bacon and Patricia Castro for guidance in 3D weak lensing and Masahiro Takada for discussions involving CMB prior estimation.

## References

- Aldering, G., 2005, *NewAR*, 49, 346
- Bassett, B., et al., 2005, *A&G*, 46e, 26
- Castro, P., Heavens, A., & Kitching, T., 2005, *Phys. Rev. D*, 72, 3516
- Eisenstein, D., Hu, W., 1998, *ApJ*, 496, 605
- Heavens, A., 2003, *MNRAS*, 343, 1327
- Heavens, A., Kitching, T., & Taylor, A., 2006, *MNRAS*, 380, 1029
- Hu, W., 2002, *Phys. Rev. D*, 65, 3003
- Jain, B. & Taylor, A. N., 2003, *Phys. Rev. Lett.*, 91, 1302
- Lamarre, J., et al., 2003, *NewAR*, 47, 1017
- Linder, E., 2003, *Phys. Rev. Lett.*, 90, 1301
- Seljak, U. & Zaldarriaga, M., 1996, *ApJ*, 469, 437
- Spergel, D., et al., 2006, *ApJS*, 177, 377
- Taylor, A., Kitching, T., Bacon, D., & Heavens, A., 2007, *MNRAS*, 2007, 374, 1377
- Taylor, A., 2005, *ADS*, pdus, confE, 28
- Wester, W., 2005, *ASPC*, 339, 152